ANL/ET/CP--82224
Conf-9410184--3

ROLE OF INTERNAL STRESSES IN FRACTURE BEHAVIOR OF ENGINEERING COMPOSITES*

J. P. Singh, D. Singh, D. S. Kupperman, and S. Majumdar

Energy Technology Division

Argonne National Laboratory

Argonne, IL 60439

May 1994

The submitted manuscript has been authored by a contractor of the U. S. Government under contract No. W-31-109-ENG-38. Accordingly, the U. S. Government retains a nonexclusive, royalty-free license to publish or reproduce the published form of this contribution, or allow others to do so, for U. S. Government purposes.

RECEIVED
OCT 14 1994
OSTI

INVITED paper to be presented at the International Symposium on High Performance Composites, October 2-6, 1994, Rosemont, IL.

*Work supported by the U.S. Department of Energy (DOE), Fossil Energy Materials Program (Advanced Research and Technology Development), and Energy Efficiency and Renewable Energy (Industrial Technologies and Utilities Technologies), under Contract W-31-109-Eng-38. This work has benefited from the use of Argonne's Intense Pulsed Neutron Source, which is supported by the DOE Office of Energy Research (Basic Energy Sciences).

MASTER

DISTRIBUTION OF THIS DOCUMENT IS UNLIMITED

DISCLAIMER

This report was prepared as an account of work sponsored by an agency of the United States Government. Neither the United States Government nor any agency thereof, nor any of their employees, make any warranty, express or implied, or assumes any legal liability or responsibility for the accuracy, completeness, or usefulness of any information, apparatus, product, or process disclosed, or represents that its use would not infringe privately owned rights. Reference herein to any specific commercial product, process, or service by trade name, trademark, manufacturer, or otherwise does not necessarily constitute or imply its endorsement, recommendation, or favoring by the United States Government or any agency thereof. The views and opinions of authors expressed herein do not necessarily state or reflect those of the United States Government or any agency thereof.

DISCLAIMER

Portions of this document may be illegible in electronic image products. Images are produced from the best available original document.

ROLE OF INTERNAL STRESSES IN FRACTURE BEHAVIOR OF ENGINEERING COMPOSITES*

J. P. Singh, D. Singh, D. S. Kupperman, and S. Majumdar

Energy Technology Division

Argonne National Laboratory

Argonne, IL 60439

ABSTRACT

Microstructure and fracture behavior of SiC(f)/Si_3N_4 matrix composites, and of Ag-particulate/$YBa_2Cu_3O_X$[YBCO] superconductor matrix composites, together with internal residual strains in composite constituents, have been evaluated as a function of reinforcing-fiber, particulate content, and processing variables. Residual strains were measured by neutron diffraction with the Intense Pulsed Neutron Source and Powder Diffractometer at Argonne National Laboratory. Internal radial strains on SiC fibers in SiC(f)/Si_3N_4 composites decreased from 0.0015 at 8.4 vol.% fibers to 0.0010 at 23.3 vol.% fibers. This decrease in radial strain with increasing fiber volume fraction is expected to reduce frictional and hence interfacial sliding stresses between SiC fibers and Si_3N_4 matrix; this is in agreement with interfacial shear strengths measured by the fiber pushout technique. Similar relationships between residual strain and interfacial shear strength was observed for composites hot isostatically pressed (HIPed). For YBCO-Ag composites, tensile strain in the Ag phase was as high as 0.085%, whereas compressive strain in the YBCO phase reached 0.09%. The presence of compressive strain (stress) improved the strength of YBCO from 200 to 223 MPa. Implications of the effects of residual stresses on interfacial characteristics and resulting composite mechanical properties and fracture behavior will be discussed.

INTRODUCTION

Ceramic composites with particulate, whisker, or continuous fiber reinforcements are becoming increasingly important structural materials because of their potentially improved mechanical properties, especially at high temperatures. The improvement in mechanical properties (especially, the fracture toughness) of the composites is believed to be due the interaction of the propagating crack with reinforcements. The toughening/strengthening mechanisms include crack deflection [1,2], microcracking [3–5], crack pinning [6], crack bridging [7,8], and fiber pullout [9]. Crack-reinforcements interactions and resulting toughening contributions depend greatly on the state of internal residual stresses induced due to the mismatch between the thermal expansion coefficients and the elastic moduli of the matrix and the reinforcing phases. Therefore, an understanding and evaluation of the role of internal stresses are critical for the development of composites with improved mechanical properties. Neutron diffraction [10,11] is a powerful technique for measuring bulk internal strains from which stresses can be calculated using appropriate stress analysis. Because neutrons can penetrate deeper than X–rays, neutron diffraction can provide a bulk measurement of strains rather than simply the surface measurement provided by X–ray diffraction. In the present paper, we present the results of bulk internal strain and stress measurements by Intense Pulsed Neutron Source (IPNS) and the General Purpose Powder Diffractometer (GPPD) at Argonne National Laboratory. The results of inernal strains/stresses were correlated with the measured mechanical properties of SiC(f)/Si_3N_4 matrix composites, and of Ag-particulate/$YBa_2Cu_3O_X$[YBCO] superconductor matrix composites.

EXPERIMENTAL PROCEDURE

Specimen Preparation and Mechanical Testing

The composite specimens used in this study included SiC(f)/Si_3N_4 and $YBa_2Cu_3O_x$ (YBCO)/Ag composites. SiC(f)/Si_3N_4 matrix composites were fabricated at NASA Lewis Research Center (Cleveland, Ohio) using commercially available SCS-6 (carbon coated) SiC monofilaments of 142 μm

diameter. The Young's modulus and Poisson's ratio for the SCS-6 filament have been reported to be 427 GPa and 0.17, respectively [12]. Transverse and longitudinal coefficients of thermal expansion of SCS-6 fibers are 2.63 x 10-6/°C and 4.5 x 10-6/°C, over the temperature ranges 0-1000°C and 50-500°C, respectively [13].

Composites, with different processing variables, were fabricated by alternatively stacking SiC fiber mats and silicon cloths in a die, followed by high-temperature consolidation and nitridation. Some of the composite SiC/RBSN specimens (with 29 vol% fiber content) were HIPed to investigate the effect of matrix densification on internal stresses and interfacial characteristics. Details of processing have been described in references [14, 15]. Table 1 lists the various composites and their associated processing variables. The elastic modulus and Poisson's ratio of the monolithic RSBN measured by ultrasonic pulse echo technique were 160 GPa and 0.2, respectively. The thermal expansion coefficient of RSBN has been reported as 3.3 x 10-6/°C [12].

Table 1. List of SiC/RBSN Composites Tested, Together with their Processing Variables

	Fiber Content	Fiber Surface	Postfabrication
Composite Type	V_f (vol.%)	Condition	Treatment
A	8–28	Carbon coated	None
B	28.9	Carbon coated	Hot isostatically pressed

For SiC(f)/Si_3N_4 matrix composites, interfacial strength between SiC(f) and Si_3N_4 matrix interface was measured by performing fiber pushout tests. Thin slices (≈0.80 mm) of composites were machined normal to the fiber axis and were ground to a surface finish of 0.25 μm. Pushout tests were performed by first locating the fibers under a tungsten carbide indenter

with a flat tip of ~60-μm-diameter attached to the top plate of the testing system. After positioning, the fibers were loaded at a constant displacement rate of 0.05 mm/min and the load-displacement behavior was continuously monitored [16] and used for the evaluation of interfacial strength.

YBCO/Ag composites were made by mixing various amounts of Ag particles with YBCO powder. The YBCO powder was made [12] by solid state reaction of Y_2O_3, BaO, and CuO. The constituent powders of Y_2O_3, $BaCO_3$, and CuO were mixed in appropriate proportions and were wet-milled in methanol for approximately 12 h. The wet-milled slurry was dried, calcined in air at 890°C for 24 h, and ground to a fine powder. Calcination and grinding were repeated three times. The final ground powder had an average particle size of ≈5μm. The YBCO–Ag composites were made [17] by mixing various amounts (10–30 vol%) of Ag powder with YBCO powder. Composite powder was used to make both rectangular bars (~5.1 x 0.6 x 0.3 cm) and extruded wires [18]. The wires were sintered at different temperatures (910–950°C) and pO_2 (0.32–760 mm Hg). The strength of wires were measured in an Instron mechanical testing machine in a three-point bending mode with a loading span of 1.825 cm and a cross head speed of 0.127 cm/min.

Bulk Internal Stress Evaluation by Neutron Diffraction Technique

The internal stresses in the composites were evaluated by first measuring lattice strain by neutron diffraction technique. Subsequently, the stresses were calculated from the measured strain values.

The neutron pulses are generated by accelerating protons to a very high energy (450 MeV) and directing them at a uranium target. Thermal neutrons with velocities up to 1000 m/s are useful for neutron diffraction experiments. At these energies, the wavelengths are on the order of lattice spacing, and Bragg's law of diffraction is applicable. Bragg's law is first used to determine the lattice spacing (d) for a particular hkl reflection from both YBCO and Ag averaged over a volume of the strain-free powder. Following the examination of the strain-free powders, the composite fabricated from the powders was examined. The lattice strain (ε) associated with the hkl plane of a given phase in the composite is given by

$$\varepsilon = (d-d_o)/d_o$$

where do is the unconstrained hkl spacing (powder) and d is the spacing for the composite. Lattice spacing can be measured to an accuracy of ±0.002 A.

RESULTS AND DISCUSSIONS

Interfacial debonding and frictional sliding stresses for composites with different processing variables were evaluated from the load-displacement plots obtained during pushout tests. Assuming a uniform distribution of stresses along the embedded fiber length, L, the interfacial debonding (τ_d) and sliding frictional (τ_f) stresses were estimated using the expression: $\tau_{d,f} = P_{d,max}/2\pi aL$ where $P_{d,max}$ corresponds to the debonding (d) or maximum pushout (max) loads, and a is the fiber radius. Table 2 shows the trends of average debonding and interfacial frictional sliding stresses for the various composites tested. The observed variations in these stresses with different processing variables including fiber content are related to the interfacial residual stresses which are discussed below.

Interfacial frictional sliding stresses are dependent on several factors such as residual stresses on the fibers and fiber surface characteristics. Decrease in frictional sliding and debonding stresses with fiber content of as-fabricated SiC/RBSN composites, as shown in Table 2, is attributed to

Table 2. Debonding and Frictional Sliding Stress of SiC/RBSN Composites Fabricated with Different Processing Variables

Composite Type	Fiber Content, V_f (vol.%)	Debonding Stress, τ_d (MPa)	Frictional Sliding Stress, τ_f (MPa)

A Reaction-Bonded	8.4	7.56 ± 1.8	7.67 ± 2.4
	12.6	13.69 ± 7.7	12.38 ± 7.7
	16.2	10.34 ± 4.5	7.88 ± 3.8
	21.7	8.22 ± 4.2	6.13 ± 3.2
	23.3	6.52 ± 2.2	5.86 ± 2.0
	27.6	8.63 ± 2.8	6.30 ± 2.6
B Reaction-Bonded and HIPed	28.9	15.30 ± 6.2	13.88 ± 7.4

changes in the residual stresses in the matrix and fiber. Based on the reported thermal expansion coefficients of fiber and matrix, it is expected that significant stresses will be generated during thermal cool-down from the composite processing temperatures. In SiC fibers, compressive stresses will be developed in transverse direction and tensile stresses will be developed along the axial direction, due to their anisotropic thermal expansion behavior. These residual stresses resist the slippage and debonding of the fiber during pushout tests. Therefore, any change in these stresses affects the maximum pushout and debonding loads, and consequently the interfacial frictional sliding and debonding stresses.

Quantitative measurements of the residual strains (stresses) in fiber and matrix of bulk SiC/RBSN composites (as-fabricated and HIPed) were conducted in the Intense Pulsed Neutron Source (IPNS) at Argonne National Laboratory and are shown in Figure 1. The figure shows variations of axial and transverse residual strains (stresses) in the fibers as a function of the fiber content. These results confirm the presence and sign of residual stresses in fibers: compressive in the transverse direction and tensile in the axial direction. In additon, with increasing fiber content the measured radial residual stresses are observed to decrease. This is agreement with

the results of measured interfacial shear strengths using pushout tests on composites with different fiber contents.

Table 2 also indicates that frictional sliding stress in HIPed composites (≈14 MPa) are twice than those in as–fabricated composites (≈7 MPa) at similar fiber contents of about 28 vol.%. Increased frictional stresses for HIPed specimens over those of as–fabricated composites can result from two causes. First, residual clamping stresses may be relatively larger in the HIPed composite because of the larger thermal cool-down from processing temperature compared to as–fabricated composites. In addition, in HIPed composites dense matrix with higher stiffness relative to as-fabricated composites results from the higher processing temperatures (≈1600°C) and pressures used. This hypotheses was confirmed by strain variation measured by IPNS on HIPed composites as shown in Fig. 1. The measured strains for

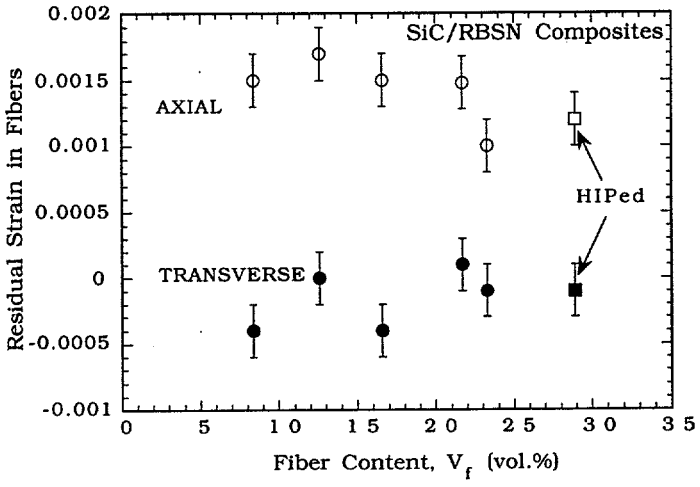

Figure 1. Measured Axial and Transverse Residual Strains in Bulk SiC/RBSN Composites with Varying Fiber Content. Solid Lines are Predictions. Residual strains were measured with the Intense Pulsed Neutron Source at Argonne National Laboratory.

HIPed composites were slightly larger than those of as-fabricated composites at comparable fiber contents indicating a presence of a larger clamping stress.

The YBCO and its composites with Ag had a density over 90% theoretical. In general, the density of the pellets increased with increasing Ag content with a density of ~95% for YBCO–30 vol.% Ag composites. The increase in density with Ag content is probably due to Ag acting as a sintering aid. A typical micrograph of the polished surface of YBCO–Ag composite is shown in Fig. 2. The micrograph clearly indicates a relatively uniform distribution of Ag in YBCO matrix. The Ag particles (white particles) are randomly distributed with little or no preferred orientation and are primarily located at the grain boundaries of YBCO grains.

Micrograph

Figure 2. Micorgraph of YBCO-Ag Composite Showing the Uniform Distribution of Ag Phase.

Table 3 shows the room–temperature average bulk strain in the Ag phase in different crystallographic orientations [19]. The results indicate that strain in Ag decreases with increasing Ag content in the composite.

Table 3. Room–temperature % tensile strain in Ag phase in different crystallographic orientations as a function of Ag content in YBCO–Ag composite

Ag Content	Lattice Plane		
(vol.%)	(111)	(200)	(220)
15	0.085±0.02	0.055±0.02	0.071±0.02
20	0.072±0.02	0.043±0.02	0.073±0.02
30	0.048±0.02	0.023±0.02	0.048±0.02

As expected, strain in the Ag phase is due to thermal expansion mismatch [19] between Ag and the YBCO–Ag composite. The average values of thermal expansion coefficient for YBCO and Ag are 16.7 x 10^{-6}/°C and19.7 x 10^{-6}/°C, respectively. The thermal expansion coefficient of YBCO–Ag composite will increase with increasing Ag content. Therefore, the thermal expansion mismatch between Ag and the YBCO–Ag composite will decrease with increasing Ag content. This will result in the observed decrease in strain in Ag phase with increasing Ag content (Table 3). However, the small difference(≈3 x 10^{-6}/°C) in the thermal expansion coefficients of YBCO and Ag is not consistent with the measured large decrease in strain in the Ag phase (Table 3). Possible mechanisms to cause this large decrease in strain are microcracking, yielding of Ag phase, and creep. Microcracking is discarded because elastic modulus should decrease if microcrack volume increases with increasing Ag content. As observed, the elastic modulus increased with increasing Ag content. An observation of the diffraction peak full–width–at–half maximum (FWHM) indicates a very small peak broadening, which suggests little or no yielding. Therefore, the rapid decrease in strain may be related to creep relaxation. As discussed before, the density of YBCO increases with increasing Ag content which may slow oxygen penetration in composites and change oxygen stoichiometry [17].

The creep of YBCO has been observed to depend on oxygen partial pressure [20]. Majumdar et al.[21] assumed that YBCO–Ag composites with different oxygen content will have different creep rates and based on the results of creep studies by Stumburg et al.[20] calculated the residual strain variation as a function of Ag content using both elastic and creep analyses. Their calculations show a better agrrement of the predicted strain variation with Ag content based on creep analysis with the measured variation than that based on elastic analysis. Therefore, the large decrease in strain with silver content can be explained in part by creep.

In order to measure strain in the YBCO phase, oxygen stoichiometry of the YBCO phase with different Ag contents was established first. This was done by comparing the diffraction peaks of YBCO in composites with those of YBCO with known stoichiometry [22]. Based on the known stoichiometry, the lattice spacing of different planes of unstrained YBCO was estimated. Subsequently, lattice spacing of the strained composites (YBCO–Ag) was measured by neutron diffraction. A comparison of the lattice spacings in the strained and unstrained conditions provided the strain in the YBCO matrix phase. The measured values of strain for (111) in YBCO matrix are shown in Table 4. The compressive strain increases with increasing Ag content for Ag contents <=20 vol.% . This is consistent with the corresponding increase in the tensile stress in the Ag phase (Table 3). At 30 vol.% Ag content, the compressive stress is considerably reduced; this is consistent with the low tensile stress in the Ag phase in the composite (Table 3). As observed in Table 4, thermal mismatch between YBCO and Ag matrix induces compressive strains in the YBCO matrix. The presence of compressive stress increased the strength of YBCO from 200 to 223 MPa as a result of 15 vol.% Ag addition.

Table 4. Estimated and experimentally measured lattice spacing and resulting compressive strain for the YBCO (111) plane as a function of Ag content

		Strain-free	Strained	
Ag content (vol.%)	YBCO stoichiometry (δ)	d_{0111} calculated (A)	d_{111} measured (A)	Strain ($\Delta d/d_0$) (%)
0	0.2	2.656	2.6559	0.00±0.03
15	0.2	2.656	2.6550	-0.04±0.03
20	0.4	2.657	2.6547	-0.09±0.03
30	0.6	2.658	2.6577	-0.01±0.03

SUMMARY

Neutron diffraction using Intense Pulse Neutron Source was succesfully used to measure bulk internal strain and stress in SiC fibers reinforced Si_3N_4 matrix composites and in Ag particulate dispersed $YBa_2Cu_3O_x$ superconductors. Internal radial strains on SiC fibers in SiC(f)/Si_3N_4 composites decreased from 0.0015 at 8.4 vol.% fibers to 0.0010 at 23.3 vol.% fibers. The decrease in radial strain with increasing fiber volume fraction leads to reduced frictional and hence interfacial sliding stresses between SiC fibers and Si_3N_4 matrix; this is in agreement with interfacial shear strengths measured by the fiber pushout technique. Measured transverse residual strains for as-fabricated RBSN composites were observed to be lower than those for HIPed composites at comparable fiber contents resulting in lower interfacial shear strengths for as-fabricated RBSN composites. For $YBa_2Cu_3O_x$ -Ag composites, the compressive strain in the

$YBa_2Cu_3O_x$ phase was as high as 0.09% which resulted in an improvement in strength of YBCO superconductors from 200 to 223 MPa.

ACKNOWLEDGMENTS

The authors wish to thank J. D. Jorgensen, H. Shaked, and J. Faber, Jr., for helpful discussions. This work was supported by the U.S. Department of Energy (DOE), Fossil Energy Materials Program (Advanced Research and Technology Development), and Energy Efficiency and Renewable Energy (Industrial Technologies and Utilities Technologies), under Contract W-31-109-Eng-38.; This work has benefited from the use of the Intense Pulsed Neutron Source at Argonne National Laboratory supported by the U. S. Department of Energy, Basic Energy Sciences.

REFERENCES

1. K. T. Faber and A. G. Evans, Acta Metall. 31 [4] 565–76 (1983).
2. K. T. Faber and A. G. Evans, Acta Metall. 31 [4] 577–84–76 (1983).
3. A. G. Evans and R. M. McMeeking, Acta Metall. 34 [12] 2435–41 (1986).
4. M. Ruhle, B. J. Dalgleish, and A. G. Evans, Scripta Metall. 21 681–86 (1987).
5. I. N. Donald and P. W. McMillan, J. Mat. Sc. 11 949–72 (1976).
6. F. F. Lange, Phil. Mag. 22 983–92 (1970).
7. A. G. Evans and K. T. Faber, J. Am. Ceram. Soc. 67 [4] 255–60 (1984).
8. T. W. Coyle, M. H. Guyot, and J. F. Jamet, Ceramic Eng. and Sc. Proc. 7 [7–8] 947–57 (1987).
9. R. W. Rice, Ceram. Eng. Sc. Proc. 2 [7–8] 667–701 (1981).

10. D. S. Kupperman, S. Majumdar, and J. P. Singh, ASME J. Eng. Mater. Technol., 112, 198–201 (1990).

11. S. Majumdar, D. S. Kupperman, and J. P. Singh, J. Am. Ceram. Soc. 71 [10] 858–63 (1988).

12. J. D. Bright, D. K. Shetty, C. W. Griffin, and S. Y. Limaye, "Interfacial Bonding and Friction in Silicon Carbide (Filament)–Reinforced Ceramic– and Glass–Matrix Composites," J. Am. Ceram. Soc., **72** [10] 1891–98 (1989).

13. R. W. Goettler and K. T. Faber, "Interfacial Shear Stresses in SiC and Al_2O_3 Fiber–Reinforced Glasses," Ceram. Eng. Sci. Proc., **9** [7–8] 861–70 (1988).

14. R. T. Bhatt, "Method of Preparing Fiber–Reinforced Ceramic Materials," U.S. Pat. No. 4689188.

15. R. T. Bhatt and J. D. Kiser, "Matrix Density Effects on the Mechanical Properties of SiC/RBSN Composites," NASA–TM–103098 (1990).

16. S. Majumdar, D. Singh, and J. P. Singh, "Analysis of Pushout Tests on an SiC–Fiber–Reinforced Reaction–Bonded Si_3N_4 Composite," Composites Engineering, **3** [4] 287–312 (1993).

17. J. P. Singh, H. J. Leu, R. B. Poeppel, E. Van Voorhees, G. T. Goudey, K. Winsley, and Donglu Shi, J. Appl. Phys. 66[7] 3154–3159 (1989).

18. S. E. Dorris, J. T. Dusek, J. J. Picciolo, R. A. Russel, J. P. Singh, and R. B. Poeppel, Proc. of Intern. Conf. on Electrical Machines, Cambridge, MA, Aug. 12–15, 1990.

19. D. S. Kupperman, J. P. Singh, J. Faber, Jr., and R. L. Hitterman, J. Appl. Phys. 66, 3396–98, (1991).

20. A. W. von Stumberg, Nan Chen, K. C. Goretta, and J. L. Routbort, J. Appl. Phys., 66, 2079–82, (1989).

21. S. Majumdar, J. P. Singh, and D. S. Kupperman, Argonne National Laboratory, Argonne, Illinois, U. S. A. and A. D. Krawitz, University of Missouri, Missouri, U. S. A., 1989, unpublished information.

22. J. D. Jorgenson, Argonne National Laboratory, Argonne, Illinois, U. S. A. private communication.